Quantum modeling, beyond secularity, of the collisional dissipation of molecular alignment using the energy-corrected sudden approximation

M. Bournazel, J. Ma, Franck Billard, Edouard Hertz, J. Wu, C. Boulet, O. Faucher, J. -M. Hartmann

▶ **To cite this version:**

M. Bournazel, J. Ma, Franck Billard, Edouard Hertz, J. Wu, et al.. Quantum modeling, beyond secularity, of the collisional dissipation of molecular alignment using the energy-corrected sudden approximation. The Journal of Chemical Physics, 2023, 158, pp.174302. ⟨10.1063/5.0150002⟩. ⟨insu-04195518⟩

HAL Id: insu-04195518

https://insu.hal.science/insu-04195518v1

Submitted on 19 May 2025

HAL is a multi-disciplinary open access archive for the deposit and dissemination of scientific research documents, whether they are published or not. The documents may come from teaching and research institutions in France or abroad, or from public or private research centers.

L'archive ouverte pluridisciplinaire **HAL**, est destinée au dépôt et à la diffusion de documents scientifiques de niveau recherche, publiés ou non, émanant des établissements d'enseignement et de recherche français ou étrangers, des laboratoires publics ou privés.

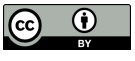

Distributed under a Creative Commons CC BY 4.0 - Attribution - International License

Quantum modeling, beyond secularity, of the collisional dissipation of molecular alignment using the energy-corrected sudden approximation

M. Bournazel[1], J. Ma[1,2], F. Billard[1], E. Hertz[1], J. Wu[2], C. Boulet[3], O. Faucher[1*], and J.-M. Hartmann[4#]

[1]Laboratoire Interdisciplinaire CARNOT de Bourgogne, UMR 6303 CNRS-Université de Bourgogne, BP 47870, 21078 Dijon, France.
[2]State Key Laboratory of Precision Spectroscopy, East China Normal University, Shanghai 200241, China.
[3]Institut des Sciences Moléculaires d'Orsay, CNRS, Université Paris-Saclay, Orsay F-91405, France.
[4]Laboratoire de Météorologie Dynamique/IPSL, CNRS, Ecole polytechnique, Institut Polytechnique de Paris, Sorbonne Université, Ecole Normale Supérieure, Université PSL, F-91120 Palaiseau, France.
[*] olivier.faucher@u-bourgogne.fr, [#] jean-michel.hartmann@lmd.ipsl.fr

ABSTRACT

We propose a Markovian quantum model for the time dependence of the pressure-induced decoherence of rotational wave packets of gas-phase molecules beyond the secular approximation. It is based on a collisional relaxation matrix constructed using the Energy Corrected Sudden approximation, which improves the previously proposed Infinite Order Sudden one by taking the molecule rotation during collisions into account. The model is tested by comparisons with time-domain measurements of the pressure-induced decays of molecular-axis alignment features (revivals and echoes) for HCl and CO_2 gases, pure and diluted in He. For the Markovian systems HCl-He and CO_2-He, the comparisons between computed and measured data demonstrate the robustness of our approach, even when the secular approximation largely breaks down. In contrast, significant differences are obtained in the cases of pure HCl and CO_2 for which the model underestimates the decay rate of the alignment at short times. This result is attributed to the non-Markovianity of HCl-HCl and CO_2-CO_2 interactions and the important contribution of those collisions that are on-going at the time when the system is excited by the aligning laser pulse.

I. INTRODUCTION

As it is well known, dissipation affects all open quantum systems interacting with an uncontrolled bath. Since this process occurs in many natural systems and practical applications, its understanding and modeling is a key issue for various scientific fields, which has stimulated large research efforts. However, the associated theoretical description is often very complex, except for extremely simple systems, due to the large numbers of quantum states and decoherence channels involved. This is why most studies use the secular approximation (SA), neglecting exchanges between density matrix elements oscillating at different frequencies, and consider that decoherence results from a succession of instantaneous and uncorrelated events, which is the Markov approximation (MA). Knowing the limits of the secular and Markovian assumptions is obviously crucial, but this requires both proper experiments and a model beyond both approximations, to analyze them.

In the particular case of collision-induced rotational decoherence addressed in this paper, studying the time-evolution of gas molecules aligned by short and intense laser pulses has proven to be a very valuable tool. Indeed, this enables to probe the field-free evolution of the system after its excitation and the creation of quantum coherences [1,2], providing quantitative information on the dissipation (see, e.g. Refs. [3-6]). By probing the dynamics at short times, using either rotational alignment revivals [1,7] or echoes [8-10], molecular alignment has recently enabled to point out the breakdown of the SA and/or MA [11,12] at the very early stage of the decoherence process. From the theoretical point of view, the first tractable quantum model was proposed, for linear molecules, in Refs. [6,13]. It uses both the SA and MA and models the state-to-state collisional rates using an Energy Corrected Sudden (ECS) approach that only depends on the principal quantum number J, thus disregarding the influence of the magnetic quantum number M. Then, a more refined M-dependent ECS approach was proposed [14], still within the MA and SA framework. Comparisons with alignment measurements over long time scales for pure CO_2 and CO_2 diluted in He [4] demonstrated the quality of this model and the need to take the influence of M into account, without which the decay of the permanent component of the alignment is strongly overestimated. This is explained [14] by the fact that, due to a gyroscopic effect, the orientation of the rotational angular momentum (quantified by M/J) is much less sensitive to collisions than the rotational speed (quantified by J). A further step was later on made [15] by extending the MA-SA-ECS model to the case of symmetric-top molecules, explicitly taking into account the influences of all (J, K, and M) rotational quantum numbers. This approach was successfully tested by comparisons with measured data for impulsively aligned Ethane gas [15]. Finally, a last progress was made in Ref. [11], where the SA was

released, and a Markovian *J*- and *M*-dependent relaxation matrix was constructed, for linear molecules, using the Infinite Order Sudden (IOS) approximation. Comparisons of the associated predictions with measurements of the alignment of N_2O diluted in He at short times (< 18 ps) demonstrated the (expected) large effects of non-secularity during the very first moments of the system's evolution. However, recall the two main limitations of Ref. [11]: the first is that the proposed IOS model assumes instantaneous intermolecular interactions and therefore disregards the rotation of the molecules during collisions. It is thus only suitable for systems (such as N_2O-He) for which: 1) the rotational constant is not too large, 2) the relative speed of interacting pairs is large, and 3) the intermolecular potential is significant only over a very narrow range of intermolecular distances. These conditions are not satisfied for most molecular systems. The second limit is that non-secular predictions could not be carried for the (room) temperature of the experiments [11], due to computer limitations resulting from excessive memory and CPU time requirements. Simulations thus had to be made at 100 K, introducing a bias in the comparison with the measured data at 295 K. Going beyond these limits is the subject of the present study, which proposes a non-secular *J*- and *M*-dependent collisional model based on the ECS approximation and tests it by comparisons with experimental values of the decay time constants of various alignment features of CO_2 and HCl, pure and diluted in He. Note that, thanks to the fact that only even *J* values exist in CO_2 while only a few *J* levels are populated for HCl, full computations for the room temperature of the experiments could be made in contrast to the non-SA simulations presented in Ref. [11].

II. EXPERIMENTAL DATA

The experimental data used in the present work for the test of the proposed model have been obtained and presented in Ref. [12]. In this previous study, four types of gas samples (CO_2 and HCl, pure and diluted in He) were excited by one (resp. two) nonresonant, short and intense laser (pump) pulses in order to generate alignment revivals for HCl (resp. alignment echoes for CO_2). The time evolution of the resulting anisotropy of the medium was then interrogated by a probe pulse providing a signal proportional to the "alignment factor", i.e. the ensemble average $\left\langle \cos^2\theta - 1/3 \right\rangle(t)$ where *t* denotes the time delay since the first pump excitation and θ is the angle between the molecular axis and the direction of the (linear) polarization of the pump pulse(s). For HCl, thanks to the small rotational period ($\simeq$1.6 ps) resulting from the large rotational constant of this molecule ($B \simeq 10$ cm^{-1}), the short-time dissipation could be directly observed by measuring the decays of the alignment revivals (at times t_R) generated by a single

pump pulse. In contrast, since CO_2 molecules rotate much slower ($B \simeq 0.39$ cm^{-1}, leading to a rotational period of $\simeq 43$ ps) than HCl, in order to access to the short-time dynamics it was necessary to align the molecule by generating a rotational echo at time $t_E = 2\tau_{12}$ which was induced by applying to the system two pump pulses separated by a time τ_{12}. This exercise was carried for each gas mixture and various total gas densities *d*. In practice, for each alignment feature appearing at $t = t_{AF}$, with $t_{AF} = t_R$, for the HCl revivals (R), or $t_{AF} = t_E$, for the CO_2 echoes (E), its density-normalized peak-to-dip amplitude $S_{Exp}(d, t_{AF})$ was determined from the recorded time-dependent alignment factor. Finally, the series of values of $S_{Exp}(d, t_{AF})$ at fixed t_{AF} was fitted by $S_{Fit}(d, t_{AF}) = A\exp[-dt_{AF}/\tau(t_{AF})]$ yielding the delay-dependent density-normalized time constant $\tau(t_{AF})$ for each considered system and alignment feature. This provided values of $\tau_R(t_R) = \tau(t_{AF})$ for the fourteen first revivals of HCl between about 1 and 12 ps, with, for the nth one $t_{AF} = t_R(n) \simeq 0.8n$ ps. For CO_2, applying several delays τ_{12} between the pump pulses enabled to obtained values of $\tau_E(2\tau_{12}) = \tau(t_{AF})$ for echoes appearing at $t_{AF} = 2\tau_{12}$ with $2\tau_{12}$ ranging from about 2 to 10 ps. These experimentally determined sets of discrete values of $\tau_R(t_R)$, for HCl, and $\tau_E(2\tau_{12})$, for CO_2, are used in the present paper to test the proposed theoretical model. Finally recall that the four mixtures studied in Ref. [12] were selected, as explained in this reference, because, in the investigated very short time scale (before about 10 ps after their excitation), they show different behaviors with respect to secularity and Markovianity: HCl diluted in He is practically secular and Markovian, while pure HCl is also practically secular but significantly non Markovian; CO_2 diluted in He is non secular but Markovian, while pure CO_2 is both non secular and non Markovian.

III. THEORETICAL MODEL AND DATA USED

The approach uses the Liouville-von Neumann equation governing the time evolution of the density matrix operator $\boldsymbol{\rho}(t)$

$$\frac{d\boldsymbol{\rho}}{dt}(t) = -\frac{i}{\hbar}[\mathbf{H}_0 + \mathbf{H}_L(t), \boldsymbol{\rho}(t)] + \left(\frac{d\boldsymbol{\rho}(t)}{dt}\right)_{Coll}, \quad (1)$$

where [**A**,**B**]=**AB**-**BA** defines the commutator between the **A** and **B** operators, $\mathbf{H}_0$ is the rotational Hamiltonian, and $\mathbf{H}_L$ describes the interaction of the molecule with the laser pulse. For a linear molecule and a laser linearly polarized, the last term takes the form

$$\mathbf{H}_{\mathrm{L}}(t) = -\frac{1}{2}\Delta\alpha E^2(t)\cos^2\theta \ , \ (2)$$

where $\Delta\alpha$ stands for the anisotropy of polarizability of the molecule and $E(t)$ is the electric field. The terms associated with the collisional dissipation are written as

$$\left(\frac{d\rho_{J'_{\mathrm{f}}M',J'_{\mathrm{i}}M'}(t)}{dt}\right)_{\mathrm{Coll}} = -d\sum_{J_{\mathrm{f}},J_{\mathrm{i}},M}\left\langle J'_{\mathrm{f}}M', J'_{\mathrm{i}}M'\middle|\mathbf{\Lambda}\middle|J_{\mathrm{f}}M, J_{\mathrm{i}}M\right\rangle\rho_{J_{\mathrm{f}}M,J_{\mathrm{i}}M}(t) \ , \ (3)$$

where $\mathbf{\Lambda}$ is the time-independent (Markovian) relaxation matrix and $\rho_{J'M,JM}(t)\equiv\left\langle J'M\middle|\boldsymbol{\rho}(t)\middle|JM\right\rangle$. Note that this expression accounts for the fact that $\mathbf{H}_0$ and $\mathbf{H}_{\mathrm{L}}$ are diagonal in M. Recall that with the non-secular approach all collisional transfers among coherences (off-diagonal elements of $\boldsymbol{\rho}$) and between populations (diagonal elements of $\boldsymbol{\rho}$) and coherences are included in Eq. (3). Removing all oscillating terms, setting $\left\langle J'_{\mathrm{f}}M', J'_{\mathrm{i}}M'\middle|\mathbf{\Lambda}\middle|J_{\mathrm{f}}M, J_{\mathrm{i}}M\right\rangle = 0$ for $J_{\mathrm{f}} \neq J'_{\mathrm{f}}$ or $J_{\mathrm{i}} \neq J'_{\mathrm{i}}$, corresponds to the SA. Once the density matrix elements are known, the time-dependent alignment factor is computed from

$$\left\langle\cos^2\theta - 1/3\right\rangle(t) = \sum_{J,M}\left\langle JM\middle|\boldsymbol{\rho}(t)\cos^2\theta\middle|JM\right\rangle = \sum_{J,M,J'}\left\langle JM\middle|\boldsymbol{\rho}(t)\middle|J'M\right\rangle\left\langle J'M\middle|\cos^2\theta\middle|JM\right\rangle \ . \ (4)$$

In order to compare calculations to experiments performed at a finite temperature, this expectation value should be computed by including all $\left|JM\right\rangle$ and $\left|J'M\right\rangle$ states of significant population before and after the pump pulse(s).

The relaxation matrix $\mathbf{\Lambda}$, describing all possible collision-induced exchanges among the density matrix elements, is here constructed beyond the previously used [11] IOS approximation as described in Appendix A. This is achieved by introducing the adiabaticity corrections [16] which (approximately) take the rotation of the molecules during collisions into account. The resulting ECS approach is thus more adapted for the description of systems involving fastly rotating molecules and/or long-lasting collisions. Recall that, while the IOS model was well adapted for N_2O diluted in He [11] (and thus also for CO_2 in He), it becomes very approximate for pure CO_2 and HCl in which the interactions between colliding pairs last much longer due to the reduced relative translational speeds and much broader ranges of distances over which the intermolecular potential is significant (see Ref. [17] for CO_2-CO_2, Ref. [18] for CO_2-He, Ref. [19] for HCl-He, and Ref. [20] for pure HCl). The ECS parameters [A, α, β and ℓ_c, see Eqs. (A7) and (A8) of Appendix A] for the four systems studied here, needed for the construction of $\mathbf{\Lambda}$, were deduced from fits of measured pressure-broadening coefficients of infrared absorption

lines for each of the considered systems. This is explained in Appendix B where their values are given and the quality of the fits is demonstrated.

Calculations with the above-described model were carried out at room temperature by including all rotational states up to J_{max}=60 for CO_2 (J_{max} =13 for HCl) a maximum quantum number for which predictions, although extremely demanding, are tractable at room temperature, contrary to the case of N_2O [11], thanks to the fact that only even J values exist in CO_2. Equation (1) was solved with a time step of 0.5 fs, starting from a Maxwell Boltzmann distribution before the laser pulse, i.e.: $\rho_{J'M,JM}(t<0^-)=\delta_{J,J'}g_J \exp(-E_J/k_BT)/Q_R(T)$ where T is the temperature, k_B is the Boltzmann constant, E_J is the energy of level J, g_J is a degeneracy factor taking into account the nuclear spin statistics when symmetric molecules are considered, and $Q_R(T)=\sum_J (2J+1)g_J \exp(-E_J/k_BT)$ is the rotational partition function. For computing Eq. (2), the polarizability anisotropies $\Delta\alpha(CO_2)=15$ a_0^3 [21] and $\Delta\alpha(HCl)=1.6$ a_0^3 [22] were used, and the laser pulse(s) characteristics were set to those of the experiments. The alignment factors [Eq. (4)] calculated for various total gas densities d were then analyzed in order to determine the density-normalized decay time constants of the revivals (for HCl) and echoes (for CO_2), exactly as done for the experiments [11, 12]). Non-secular calculations were performed by using a full relaxation matrix $\mathbf{\Lambda}$, and, in order to test the limits of the SA, secular computations were also made by setting to zero all the non-diagonal elements $\langle J'_f M', J'_i M' | \mathbf{\Lambda} | J_f M, J_i M \rangle$ for which the involved rotational energies verify $E_{J_f} - E_{J_i} \neq E_{J'_f} - E_{J'_i}$, i.e.: $J_f \neq J'_f$ or $J_i \neq J'_i$.

IV. RESULTS AND DISCUSSION

The theoretical results are compared with the measured density-normalized decay time constants of Ref. [12] in Figs. 1 and 2 for the four studied systems. Recall that amagat units of density are such that 1 amagat corresponds to 2.686 10^{25} molecule.m^{-3}. Let us emphasize that, since the input data used for the calculations have been determined (see Appendix B) completely independently of the experimental results displayed in these figures, the tests presented thereafter are unbiased and meaningful. Furthermore, recall that the secular approximation breaks down at short times but then becomes progressively valid as the dephasings between the density matrix elements wich oscillate at different frequencies increase. This occurs for delays that are inversely proportional to the considered molecule rotational constant B [11, 12]. As a result, HCl ($B \simeq 10$

cm^{-1}) has a behavior that becomes well modeled by the SA much sooner after the laser excitation than CO_2 ($B \simeq 0.39$ cm^{-1}), as demonstrated below and in Ref. [12].

Figure 1 displays the results obtained for CO_2 and HCl diluted in He, which are both Markovian systems [12]. As can be seen, the behavior of CO_2-He in Fig. 1(a) is close to that of the very similar N_2O-He system [11] with a significant decrease of the measured decay time constant with the delay in the considered time range, and values that asymptotically tend toward a constant value at long times (the plateau region). This behavior is very well reproduced by the ECS model when non-secular effects are taken into account but not when the SA is used. In this latter case, the decay rates are significantly overestimated at early times because the collision-induced exchanges between the density matrix elements wich oscillate at different frequencies, which slow down the decoherence process, are then neglected. At longer times, the SA becomes valid and the two calculations, as well as the measured values, are expected to reach (likely after a few tens of ps) the same plateau value expected, from a visual extrapolation of Fig. 1(a), to be around 75 ps.amagat. For HCl diluted in He, the comparisons between the non-secular and secular theoretical results in Fig. 1(b) confirm that the SA becomes valid much sooner than for CO_2 due to the higher rotational constant and associated much quicker increase with time of the dephasing between the density matrix elements oscillating at different frequencies. Again, using the SA leads to overestimated decays of the revivals at early times. Unfortunately, and in contrast with the measured data for the other systems studied, the large uncertainties of the experimental values for HCl-He, which are explained in the Appendix of Ref. [12], do not enable to discriminate the two models for this system.

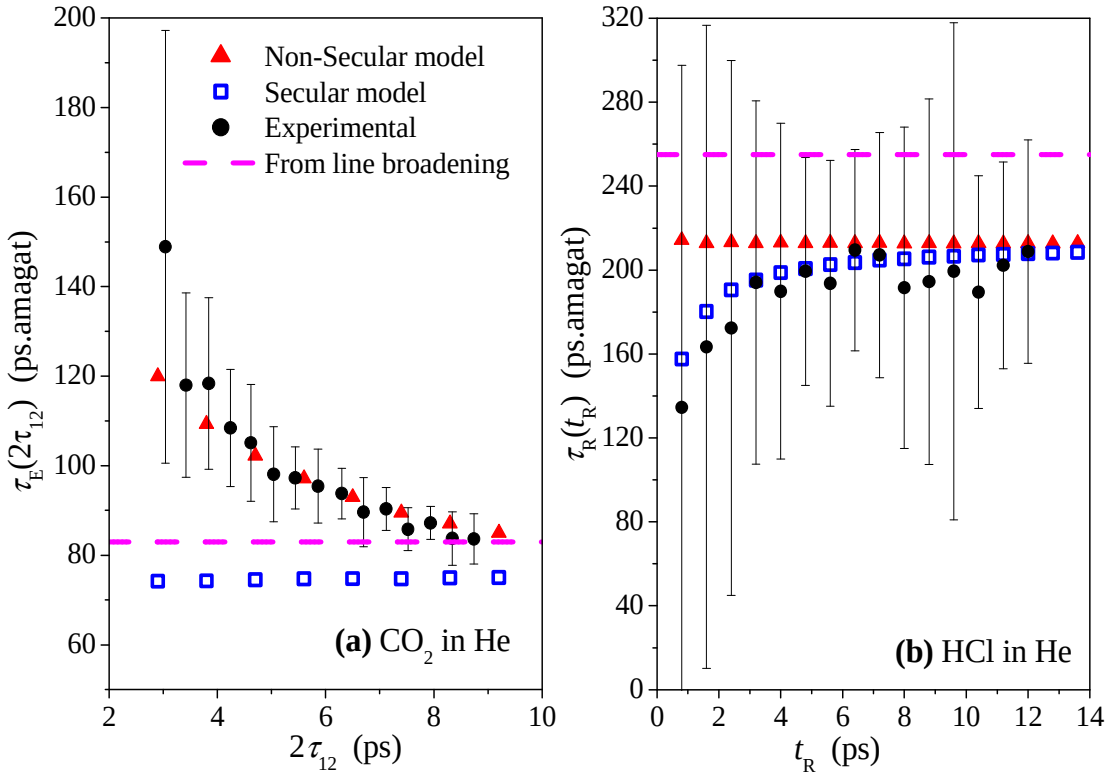

Fig. 1: Density-normalized time constants of the decays of echoes of CO_2 (a) and revivals of HCl (b), both infinitely diluted in He, as a function of their times of appearance, respectively t_R and $2\tau_{12}$ after the (first) laser excitation. The black full circles with error bars are the experimental values from Ref. [12], while the blue open squares and red full triangles represent the predictions obtained using a secular and non-secular approach, respectively. The horizontal dashed magenta lines indicate the values of the population weighted average of the measured pressure-broadening coefficient of infrared absorption lines from Ref. [23] for CO_2-He and Ref. [24] for HCl-He (displayed in Appendix B).

The results for pure HCl, whose behavior quickly becomes secular as demonstrated above and for which large and persistent non-Markovian effects exist [12] due to the strong and long-range dipole-dipole forces in colliding pairs are displayed in Fig. 2(a). Comparisons between the two calculations confirm the quickly vanishing non-secularity observed in Fig. 1(b) and the large influence of non-Markovianity. The latter strongly quickens the decoherence at early times, a behavior demonstrated [12] using molecular dynamics simulations and explained by the important role played by those molecules which are interacting with an other at the time (t=0) of the laser excitation. As discussed in Ref. [12], these collisions induce much quicker rotational exchanges than at long time scales where the decoherence becomes governed by the mean time interval between (efficient) collisions. This, which can be neglected for collisions with He, lasts for typically 1/2 ps in the cases of pure CO_2 and HCl, a value consistent with the collision

duration estimated from $\Delta R / \overline{v}_r$ for the typical values of the interaction potential range $\Delta R = 3$ Å and mean relative speed $\overline{v}_r$ =600 m/s. Despite the shortness of this effect, its influence on the decoherence process is only forgotten after a few tens of ps, delay over which the system keeps the memory of this "initial" fast decay. This is not considered by the present Markovian ECS model which thus significantly overestimates the decay time constants during a few tens of ps before the plateau region (not shown) where the system behavior becomes well modeled by the Markov (and secular) approach. The results for pure CO_2 (a significantly non-secular and non-Markovian system [12]) are displayed in Fig. 2(b). They show that, as for pure HCl, the non-secular ECS predictions overestimate the decay time constant because non-Markovian effects are disregarded by this model. As analyzed in Ref. [12], non-secularity and non-Markovianity have opposite influences (they respectively slow-down and accelerate the early dissipation) which, for pure CO_2, tend to compensate each other, reducing the temporal variation of the decay time constants, in contrast with those for CO_2 diluted in He.

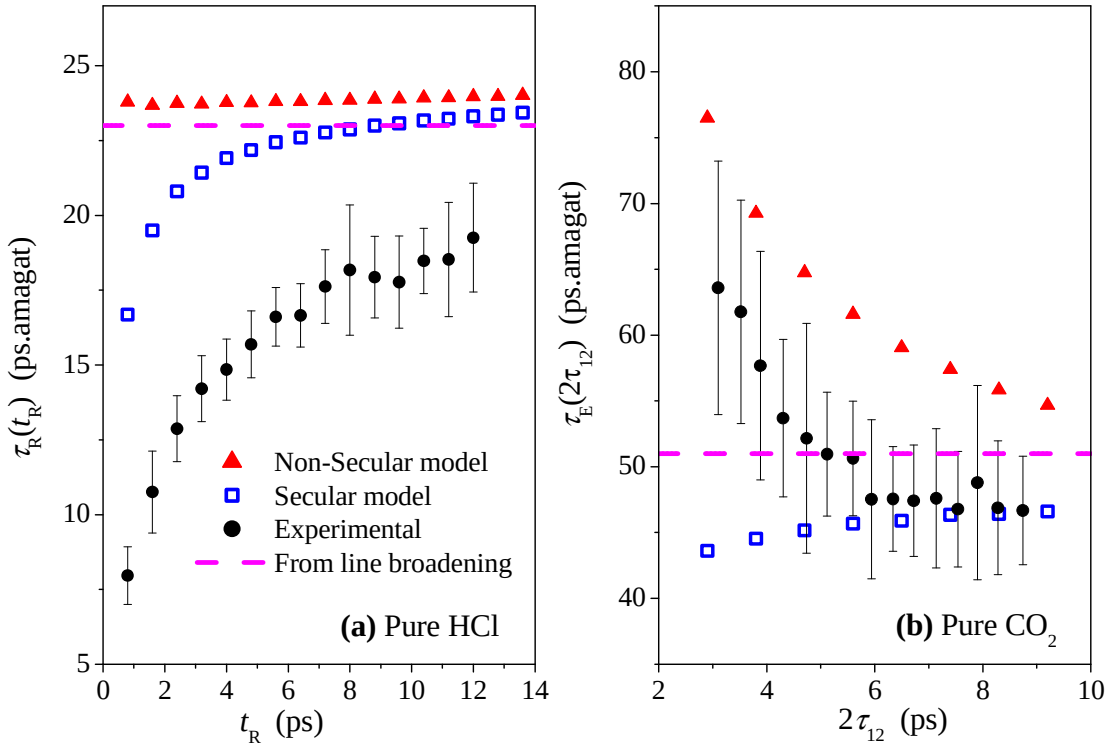

Fig. 2: Density-normalized time constants of the decays of the revivals of pure HCl (a) and echoes of pure CO_2 (b), as a function of their times of appearance, respectively t_R and $2\tau_{12}$ after the (first) laser excitation. The black full circles with error bars are the experimental values from Ref. [12], while the blue open squares and red full triangle represent the predictions obtained using a secular and non-secular approach, respectively. The horizontal dashed magenta lines indicate the values of the population weighted average of the measured pressure-broadening

coefficient of infrared absorption lines from Ref. [25] for pure CO_2 and Ref. [26] for pure HCl (displayed in Appendix B).

For comparison with the alignment decay time constants, it is of interest to consider the pressure-broadening coefficients γ of the absorption lines which monitor [27] the (exponential) decay of the autocorrelation function of the molecular dipole $\vec{\mu}(t)$ at long times that is due to the collision-induced decoherence of the molecular axis rotation. This Markovian and secular quantity thus has much in common with the alignment decay rates that would be observed at long time delays when the plateau region is reached and the SA and MA both become valid. This statement is confirmed by the horizontal dashed lines in Figs. 1 and 2 which display the values of $\tau_{\overline{\gamma}} = 1/(2\pi c\overline{\gamma})$, where c (in cm.s^{-1}) is the speed of light and $\overline{\gamma}$ (in cm^{-1}.amagat^{-1}) is the population-weighted averaged value of the measured individual line-broadening coefficients displayed in Fig. B1 of Appendix B.

V. CONCLUSION

We have proposed a Markovian quantum approach based on the Energy Corrected extension of the Infinite Order Sudden model for calculations of the collision-induced decoherence of molecular rotational wave packets that takes non-secular effects into account. It has been tested by comparisons with time-domain experimental results for molecules (HCl and CO_2, pure and diluted in He) aligned by intense and short laser pulse(s). This demonstrated a very good agreement for collisions with He (which involve Markovian processes) even when significant non-secular effects, which slow down the dissipation process, are involved. As expected, significant differences between measured and predicted values are obtained when non-Markovianity plays a large role at the early times of the system evolution. Indeed, the decay times constants for pure HCl and CO_2 are then significantly overestimated since the influence of those collisions that are on-going when the system is excited is not considered. After the progress made in Refs. [13,14,15,11] (in chronological order) in the quantum modeling of the pressure-induced dissipation of molecular alignment, the present paper provides a further step by proposing a non-secular and non-sudden (but Markovian) approach suitable for gas-phase systems involving molecules whose rotation during collisions cannot be neglected. However, the crucial issue of developing a tractable quantum model beyond the Markov framework remains to be solved. This is a very complex problem for which a solution may be brought by (requantized) classical molecular dynamics simulations (rCMDS) which were shown to accurately describe the

influence of non-Markovianity on the collisional dissipation of laser-induced alignment [12] as well as on the line-core and -wing regions of pressure-broadened light-absorption spectra (e.g. Refs. [31-34]). One could determine, from the rCMDS, the time dependence of the basic rates $Q_L(t)$ from the evolution with time of $N(J=0, J=L, t)/N(J=0, J=0, t=0)$ where $N(J=0, J=L, t)$ is the number of molecules within the J=0 level at t=0 which have been transferred, by collision(s), to the J=L level at time t. Introducing these $Q_L(t)$'s into the equations of Appendix A would, in principle, enable to construct a time-dependent relaxation matrix $\mathbf{\Lambda}(t)$ then taking into account the influence of the initially on-going collisions.

ACKNOWLEDGEMENTS

The work was supported by the Conseil Régional de Bourgogne Franche-Comté, the CNRS, EIPHI (Engineering and Innovation through Physical Sciences, High-technologies, and cross-dIsciplinary research) Graduate School (Grant No. ANR-17-EURE-0002) and has benefited from the facilities of the SMARTLIGHT platform in Bourgogne Franche-Comté (Grant No. ANR-21-ESRE-0040). J. Ma acknowledges the support from the China Scholarship Council (CSC). J.-M. Hartmann benefited, for the computer simulations, from the IPSL mesocenter ESPRI facility. J. Wu acknowledges the support by the National Key R&D Program (Grant No. 2018YFA0306303) and the NSFC (Grant No. 11834004).

AUTHOR DECLARATIONS

Conflict of Interest

The authors have no conflicts to disclose.

Author Contributions

M. Bournazel: Investigation (equal); Formal analysis (equal); Validation (equal); Writing - review and editing (equal). **J. Ma:** Investigation (equal); Formal analysis (equal); Validation (equal); Writing - review and editing (equal). **F. Billard:** Investigation (equal); Software (equal); Writing - review and editing (equal). **E. Hertz:** Funding acquisition (equal); Writing - review and editing (equal). **J. Wu**: Funding acquisition (equal); Writing - review and editing (equal). **C. Boulet:** Methodology (equal); Software (equal); Writing - review and editing (equal). **O. Faucher:** Conceptualization (equal); Supervision (equal), Project administration (equal); Funding acquisition (equal); Review and editing (equal). **J.-M. Hartmann:** Conceptualization (lead); Formal analysis (lead); Methodology (lead); project administration (lead); supervision (lead); Software (equal); Visualization (lead); Writing – original draft (lead); Writing – review and editing (equal).

DATA AVAILABILITY

The data that support the findings of this study are available from the corresponding author upon reasonable request.

APPENDICES

A. The Energy Corrected Sudden collisional relaxation matrix

In Ref. [11], a model based on the Infinite Order Sudden (IOS) approximation was proposed to construct the Markovian relaxation matrix $\mathbf{\Lambda}$ beyond the secular approximation. The IOS model, which disregards the rotation of the molecule during collisions (which explains the "Sudden" denomination) was adapted for the considered N_2O-He collisional pair due to the extreme shortness of intermolecular interactions (as for CO_2-He). This is not the case for pure CO_2 and HCl considered in the present study which involve much longer lasting intermolecular forces (due to both the extended potential range and slower relative speeds of the collision partners). To overcome this limitation, we first introduce the corrections proposed in Ref. [16], which leads to the following Energy Corrected Sudden expression [14]:

$$\left\langle J'_{\rm f}\, M', J'_{\rm i}\, M' \middle| \mathbf{\Lambda} \middle| J_{\rm f} M, J_{\rm i} M \right\rangle = -\frac{\rho_0(J_>)}{\rho_0(J_i)} \sqrt{(2J_{\rm i}+1)(2J'_{\rm i}+1)(2J_{\rm f}+1)(2J'_{\rm f}+1)} \times \sum_L \begin{pmatrix} J_{\rm f} & J'_{\rm f} & L \\ 0 & 0 & 0 \end{pmatrix} \begin{pmatrix} J_{\rm i} & J'_{\rm i} & L \\ 0 & 0 & 0 \end{pmatrix} \begin{pmatrix} J_{\rm f} & J'_{\rm f} & L \\ M & -M' & M'-M \end{pmatrix} \begin{pmatrix} J_{\rm i} & J'_{\rm i} & L \\ M & -M' & M'-M \end{pmatrix} \frac{\Omega(J_>, \ell_{\rm c})(2L+1)Q_L}{\Omega(L, \ell_{\rm c})} \quad , \text{(A1)}$$

where the Q_L's are basic collisional rates and $\Omega(J, \ell_c)$ is the adiabaticity factor [16], which are discussed later. $\rho_0(J_>)/\rho_0(J_i) = \exp(-E_{J_>}/k_BT)/\exp(-E_{J_i}/k_BT)$, with $J_> \equiv \sup(J_i, J'_i)$, ensures that the following detailed balance relation:

$$\left\langle J'_{\rm f}\, M', J'_{\rm i}\, M' \middle| \mathbf{\Lambda} \middle| J_{\rm f} M, J_{\rm i} M \right\rangle \rho_0(J_{\rm i}) = \left\langle J_{\rm f} M, J_{\rm i} M \middle| \mathbf{\Lambda} \middle| J'_{\rm f}\, M', J'_{\rm i}\, M' \right\rangle \rho_0(J'_{\rm i}) \quad \text{(A2)}$$

is verified by Eq. (A1).

At this step, two difficulties remain. The first one, well known from spectroscopic studies of line-mixing effects (Sec. IV.3.3 of Ref. [27]), is that Eq. (A1) cannot be used when the $Q_{L=0}$ term is involved in the sum over L which is here the case, according to the selection rule of the 3J symbols, when $J'_{\rm i} = J_{\rm i}$, $J'_{\rm f} = J_{\rm f}$, and $M' = M$. This corresponds to two types of terms:

(i) The first kind, for $J'_{\rm i} = J_{\rm i} = J'_{\rm f} = J_{\rm f} = J$ and $M' = M$, is associated with the diagonal element of $\mathbf{\Lambda}$ governing the loss of the population $\langle JM | \boldsymbol{\rho} | JM \rangle$. Equation (A1) does not apply, but the following exact relation:

$$\left\langle JM, JM \middle| \mathbf{\Lambda} \middle| JM, JM \right\rangle = \sum_{(J',M') \neq (J,M)} K(JM \to J'M') \quad , \text{(A3)}$$

connecting the $\left\langle JM, JM \middle| \mathbf{\Lambda} \middle| JM, JM \right\rangle$ element to the $K(JM \to J'M')$ state-to-state rates can be used since the latter can be computed within the ECS approximation using Eq. (C2) of Ref. [14]. Incidentally note that $\left\langle J'M', J'M' \middle| \mathbf{\Lambda} \middle| JM, JM \right\rangle = -K(JM \to J'M')$.

(ii) The second kind of terms, which correspond to $J'_{\rm i} = J_{\rm i}$, $J'_{\rm f} = J_{\rm f}$ and $M' = M$, is associated with the loss of the $\langle J_{\rm f} M | \boldsymbol{\rho} | J_{\rm i} M \rangle$ coherence. Again, Eq. (A1) does not apply, but an exact relation can be used [13,14], relating $\langle J_{\rm f} M, J_{\rm i} M | \boldsymbol{\Lambda} | J_{\rm f} M, J_{\rm i} M \rangle$ to the state-to-state rates introduced above and to a pure dephasing contribution $\gamma^{\rm PD}_{J_{\rm i} M, J_{\rm f} M}$, i.e.:

$$\langle J_{\rm f} M, J_{\rm i} M | \boldsymbol{\Lambda} | J_{\rm f} M, J_{\rm i} M \rangle = \gamma^{\rm PD}_{J_{\rm i} M, J_{\rm f} M} + \frac{1}{2} \sum_{(J',M') \neq (J_{\rm i}, M)} K(J_{\rm i} M \rightarrow J' M') + \frac{1}{2} \sum_{(J',M') \neq (J_{\rm f}, M)} K(J_{\rm f} M \rightarrow J' M') \quad , \text{(A4)}$$

where $\gamma^{\rm PD}_{J_{\rm i} M, J_{\rm f} M}$ can be computed using the IOS expression given in Eq. (16) of Ref. [14] (although their relative contributions to the dissipation of the alignment turn out to be very small [14]).

The second difficulty is that the terms coupling populations and coherences [$\langle J'_{\rm f} M', J'_{\rm i} M' | \boldsymbol{\Lambda} | J_{\rm i} M, J_{\rm i} M \rangle$ and $\langle J_{\rm i} M, J_{\rm i} M | \boldsymbol{\Lambda} | J'_{\rm f} M', J'_{\rm i} M' \rangle$] constructed using Eq. (A1) verify the detailed balance relation in Eq. (A2), but not the following exact one [28,29]:

$$\langle J_{\rm i} M, J_{\rm i} M | \boldsymbol{\Lambda} | J'_{\rm f} M', J'_{\rm i} M' \rangle = \langle J'_{\rm f} M', J'_{\rm i} M' | \boldsymbol{\Lambda} | J_{\rm i} M, J_{\rm i} M \rangle \rho_0(J_{\rm i}) \quad . \text{(A5)}$$

The solution to this problem that we propose uses two steps: We first calculate the coupling $\langle J'_{\rm f} M', J'_{\rm i} M' | \boldsymbol{\Lambda} | J_{\rm i} M, J_{\rm i} M \rangle$ between population (right) and coherence (left) by using Eq. (A1) without the $\rho_0(J_>)/\rho_0(J_i)$ factor. Then the transposed term $\langle J_{\rm i} M, J_{\rm i} M | \boldsymbol{\Lambda} | J'_{\rm f} M', J'_{\rm i} M' \rangle$ is obtained from the latter by using Eq. (A5).

Note that one can show that the here proposed ECS model does verify the following exact sum rule [28,29]:

$$\sum_{J_{\rm i}, M} \langle J'_{\rm f} M', J'_{\rm i} M' | \boldsymbol{\Lambda} | J_{\rm i} M, J_{\rm i} M \rangle \rho_0(J_{\rm i}) = 0 \quad , \text{(A6)}$$

which plays a major role because it ensures that, in the absence of any laser excitation, the density matrix computed using Eqs. (1) and (3) of the main text remains at all times that of a system at Boltzmann equilibrium, since one then has $(d\boldsymbol{\rho}(t)/dt)_{Coll} = 0$.

Let us now turn back to the adiabaticity factor $\Omega(J, \ell_c)$ and basic rates Q_L which are the ingredients needed for the construction of $\boldsymbol{\Lambda}$. For the first, which approximately accounts for the influence of the molecule rotation during collisions, the following expression was proposed [16] for molecule-atom interactions, parameterized by a "scaling length" ℓ_c:

$$\Omega(J,\ell_c)=[1+(\omega_{J,J-\Delta J}\times\ell_c/\overline{v}_{\rm r})^2/24]^{-2}\ , \text{(A7)}$$

where $\omega_{J,J-\Delta J}=(E_J-E_{J-\Delta J})/\hbar$ is obtained from the energy difference between the rotational level J and the nearest inferior level significantly coupled to J by the intermolecular potential (i.e. J-2 and J-1 for CO_2 and HCl, respectively), and $\overline{v}_{\rm r}$ denotes the mean relative speed for the considered temperature and collisional pair (note that $\ell_c/\overline{v}_{\rm r}$ is a typical collision duration). We here propose a slight change in order to approximately take into account, for pure HCl, the resonance effects in simultaneous rotational-state changes within pairs of interacting molecules. It simply consists in using $\omega_{J,J-\Delta J}=(E_J-E_{J-\Delta J})/\hbar-(E_{J_{\rm max}}-E_{J_{\rm max}-\Delta J})/\hbar$ where $J_{\rm max}$ is the rotational quantum number of the most populated level. For the Q_L's, which can be identified as being the rates for the collisional de-excitation from level $J = L$ to $J = 0$, they can, in principle, be obtained from quantum scattering calculations provided that an intermolecular potential is available. In the absence of such computations, the approach, widely used for computations of pressure effects on molecular absorption spectra (see Sec. IV.3.3 of Ref. [27]), consists in using an empirical modeling such as the exponential-power law:

$$Q_{L\neq 0}=A\left[L(L+1)\right]^{-\alpha}\exp(-\beta E_L/k_{\rm B}T)\ , \text{(A8)}$$

where E_L is the rotational energy of level $J=L$, T is the temperature, and $k_{\rm B}$ is the Boltzmann constant. Equations (A7) and (A8) show that the relaxation matrix for a given collisional pair and temperature can be constructed when the A, α, β and ℓ_c parameters are known. The following Appendix explains how their values for the systems considered in this study were determined.

B. Determination of the Energy Corrected Sudden model parameters

As widely done in frequency-domain studies of "line-mixing" effects (which is how the spectroscopic community names non-secularity effects) on molecular spectra, the values of the A, α, β, and ℓ_c parameters have been determined from fits of measured pressure-broadening coefficients $\gamma_{J_{\rm f}J_{\rm i}}$ of the $J_{\rm f}\leftarrow J_{\rm i}$ optical transitions. This is made possible by the fact that one has the sum rule [27]:

$$\gamma_{J_{\rm f}J_{\rm i}}=\langle J_{\rm f}J_{\rm i}|\mathbf{W}|J_{\rm f}J_{\rm i}\rangle=-\frac{1}{\langle J_{\rm f}|\mathbf{d}|J_{\rm i}\rangle}\sum_{(J'_{\rm f},J'_{\rm i})\neq(J_{\rm f},J_{\rm i})}\langle J'_{\rm f}|\mathbf{d}|J'_{\rm i}\rangle\langle J'_{\rm f}\,J'_{\rm i}|\mathbf{W}|J_{\rm f}J_{\rm i}\rangle\ , \text{(B1)}$$

where, for the infrared line-broadening data used below, the dipole reduced matrix element $\langle J_{\rm f}|\mathbf{d}|J_{\rm i}\rangle$ is:

$$\langle J_f | \mathbf{d} | J_i \rangle = (-1)^{J_f} \sqrt{2J_f+1} \begin{pmatrix} J_f & 1 & J_i \\ 0 & 0 & 0 \end{pmatrix}, \quad \text{(B2)}$$

and the off-diagonal elements of the spectroscopic relaxation matrix **W** within the ECS approach are given by:

$$\langle J'_f \; J'_i | \mathbf{W} | J_f \, J_i \rangle = - \frac{\rho_0(J_>)}{\rho_0(J_i)} \Omega(J_>, \ell_c)(2J_< +1) \sqrt{(2J_f+1)(2J'_f+1)} \times \sum_{L \neq 0} \begin{pmatrix} J'_i & L & J_i \\ 0 & 0 & 0 \end{pmatrix} \begin{pmatrix} J'_f & L & J_f \\ 0 & 0 & 0 \end{pmatrix} \begin{Bmatrix} J_i & J_f & 1 \\ J'_f & J'_i & L \end{Bmatrix} \times (2L+1) \frac{Q_L}{\Omega(L, \ell_c)} \quad \text{. (B3)}$$

The values of A, α, β, and ℓ_c for the system studied here were obtained from fits of measured line-broadening coefficients using Eqs. (A7), (A8), and (B1)-(B3). They are given in table 1 below (incidentally note that our values of the ECS parameters for pure HCl are in very good agreement with those determined from double resonance experiments in Ref. [30]), Fig. 3 showing that they lead to good agreements between the ECS computed line broadening coefficients and the input measured data. Furthermore, recall that, as well known [27], line-broadening coefficients $\gamma_{J_f J_i}$ computed using the IOS approximation [with assumes $\ell_c = 0$ and thus $\Omega(J, \ell_c) = 1$] are practically constant and independent of J_i and J_f. Figure B1 shows that this is consistent with measured data for CO_2-He but not at all for the other systems considered in this study, for which ECS corrections are obviously needed.

	$10^3 A$ cm^{-1}/amagat	α	$10^3 \beta$	ℓ_c Å
CO_2-CO_2	38.	0.89	9.	1.80
CO_2-He	42.	1.05	40.	0.71
HCl-HCl	56.	0.	2550.	0.86
HCl-He	10.	1.00	1.5	0.40

Table 1: Parameters of the ECS model, used in Eqs. (A7) and (A8).

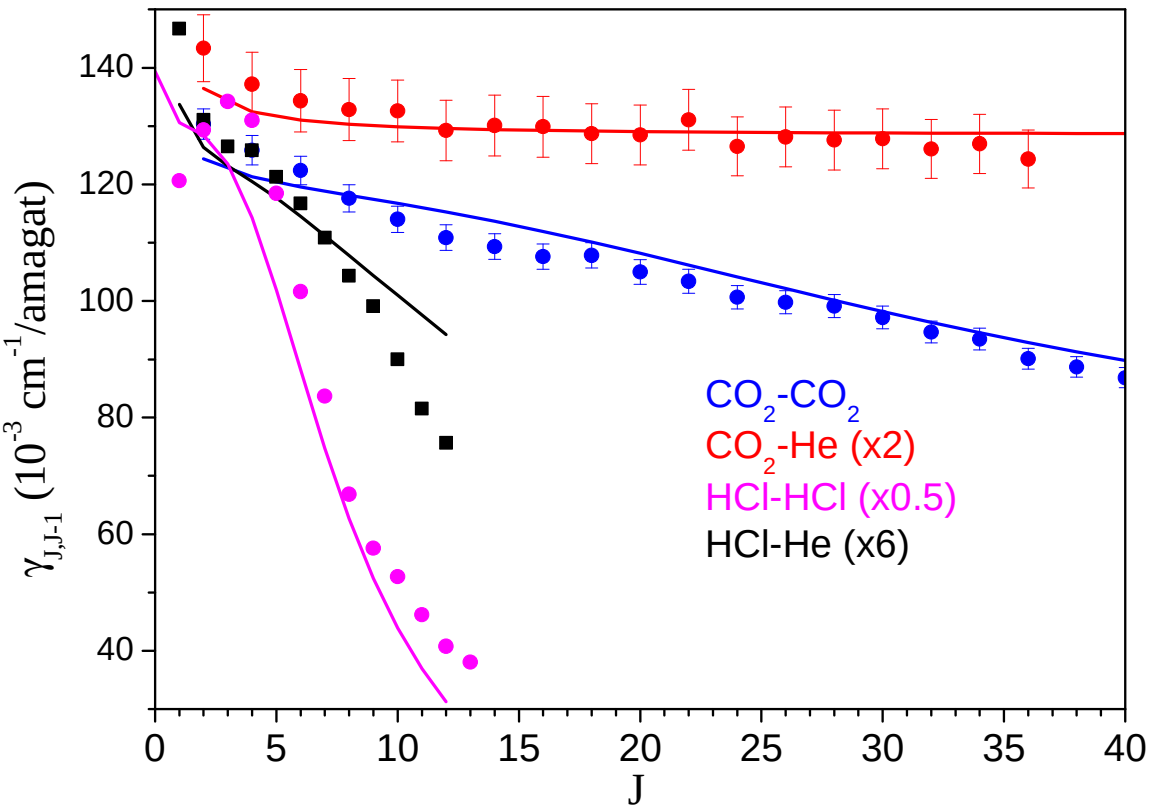

Figure 3: Measured (symbols) and ECS-computed (lines) pressure-broadening coefficients (Half Width at Half Maximum) of R(*J*) lines of CO_2 broadened by CO_2 (measurements from Ref. [25]), of CO_2 broadened by He (multiplied by 2, measurements from Ref. [23]), of HCl broadened by HCl (divided by 2, measurements from Ref. [26]), and of HCl broadened by He (multiplied by 6, measurements from Ref. [24]).

REFERENCES

1 H. Stapelfeldt and T. Seideman, Rev. Mod. Phys. **75**, 543 (2003).
2 P. M. Felker, J. S. Baskin, and A. H. Zewail, J. Phys. Chem. **90**, 724 (1986).
3 N. Owschimikow, F. Königsmann, J. Maurer, P. Giese, A. Ott, B. Schmidt, and N. Schwentner, J. Chem. Phys. **133**, 044311 (2010).
4 T. Vieillard, F. Chaussard, F. Billard, D. Sugny, O. Faucher, S. Ivanov, J.-M. Hartmann, C. Boulet, and B. Lavorel, Phys. Rev. A **87**, 023409 (2013).
5 H. Zhang, F. Billard, X. Yu, O. Faucher, and B. Lavorel, J. Chem. Phys. **148**, 124303 (2018).
6 S. Ramakrishna and T. Seideman, Phys. Rev. Lett. **95**, 113001 (2005).
7 K. Lin, I. Tutunnikov, J. Ma, J. Qiang, L. Zhou, O. Faucher, Y. Prior, I. S. Averbukh, and J. Wu, Adv. Photonics **2**, 024002 (2020).
8 G. Karras, E. Hertz, F. Billard, B. Lavorel, J.-M. Hartmann, O. Faucher, E. Gershnabel, Y. Prior, and I. S. Averbukh, Phys. Rev. Lett. **114**, 153601 (2015).
9 K. Lin, P. Lu, J. Ma, X. Gong, Q. Song, Q. Ji, W. Zhang, H. Zeng, J. Wu, G. Karras, G. Siour, J.-M. Hartmann, O. Faucher, E. Gershnabel, Y. Prior, and I. S. Averbukh, Phys. Rev. X **6**, 041056 (2016).
10 D. Rosenberg, R. Damari, and S. Fleischer, Phys. Rev. Lett. **121**, 234101 (2018).
11 J. Ma, H. Zhang, B. Lavorel, F. Billard, E. Hertz, J. Wu, C. Boulet, J.-M. Hartmann, and O. Faucher, Nature Comm. **10**, 5780 (2019).
12 M. Bournazel, J. Ma, F. Billard, E. Hertz, J. Wu, C. Boulet, J.-M. Hartmann, and O. Faucher, Phys. Rev. A **107**, 023115 (2023).
13 S. Ramakrishna and T. Seideman, J. Chem. Phys. **124**, 034101 (2006).
14 J.-M. Hartmann and C. Boulet, J. Chem. Phys. **136**, 184302 (2012).
15 J.-M. Hartmann, C. Boulet, H. Zhang, F. Billard, O. Faucher, and B. Lavorel, J. Chem. Phys. **149**, 214305 (2018).
16 A. E. DePristo, S. T. Augustin, R. Ramaswamy, and H. Rabitz, J. Chem. Phys. **71**, 850 (1979).
17 S. Bock, E. Bich, and E. Vogel, Chem. Phys. **257**, 147 (2000).
18 T. Korona, R. Moszynski, F. Thibault, J.-M. Launay, B. Bussery-Honvault, J. Boissoles, and P. E. S. Wormer, J. Chem. Phys. **115**, 3074 (2001).
19 Y. Ajili, K. Hammami, N. E. Jaidane, M. Lanza, Y. N. Kalugina, F. Lique, and M. Hochlaf, Phys. Chem. Chem. Phys. **15**, 10062 (2003).
20 P. K. Naicker, A. K. Sum, and S. I. Sandler, J. Chem. Phys. **118**, 4086 (2003).
21 A. P. Kouzov and M. Chrysos, Phys. Rev. A **80**, 042703 (2009).
22 G. Maroulis, J. Chem. Phys. **108**, 5432 (1998).
23 F. Thibault, J. Boissoles, R. Le Doucen, J.-P. Bouanich, Ph. Arcas, and C. Boulet, J. Chem. Phys. **96**, 4945 (1992).
24 G. Li, R. E. Asfin, A. V. Domanskaya, and V. Ebert, Mol. Phys. **116**, 3495 (2018).
25 A. Predoi-Cross, A. V. Unni, W. Liu, I. Schofield, C. Holladay, A. R. W. McKellar, and D. Hurtmans, J. Mol. Spectrosc. **245**, 34 (2007).
26 A. S. Pine, J. Mol. Spectrosc. **114**, 148 (1985).
27 J.-M. Hartmann, C. Boulet, and D. Robert, *Collisional Effects On Molecular Spectra. Laboratory experiments and models, consequences for applications* (2nd edition), (Elsevier, Amsterdam, 2021).
28 A. G. Redfield, IBM J. Res. Dev. **1**, 19 (1957).
29 R. Joynt, B. H. Nguyen, and V. H. Nguyen, Adv. Nat. Sci.: Nanosci. and Nanotech. **1**, 02301 (2010).
30 F. Menard-Bourcin, T. Delaporte, and J. Menard, J. Chem. Phys. **84**, 201 (1986).
31 J.-M. Hartmann, C. Boulet, H. Tran, and M. T. Nguyen, J. Chem. Phys. **133**, 144313 (2010).
32 H. Tran, G. Li, V. Ebert, and J.-M. Hartmann, J. Chem. Phys. **146**, 194305 (2017).

33 Z. Reed, H. Tran, N. H. Ngo, J.-M. Hartmann, and J. T. Hodges, Phys. Rev. Lett. **130**, 143001 (2023).
34 H. Tran, G. Li, N. H. Ngo, and V. Ebert, Phys. Chem. Chem. Phys., “Advance Article” available at https://doi.org/10.1039/D2CP04892B (2023).